Applied Physics Letters

RESEARCH ARTICLE | MARCH 19 2009

Observation of stacking faults formed during homoepitaxial growth of *p*-type $4H$-SiC

Ho Keun Song; Jeong Hyun Moon; Hyeong Joon Kim; Mehran Mehregany

Appl. Phys. Lett. 94, 112109 (2009)
https://doi.org/10.1063/1.3089697

18 May 2024 09:54:08

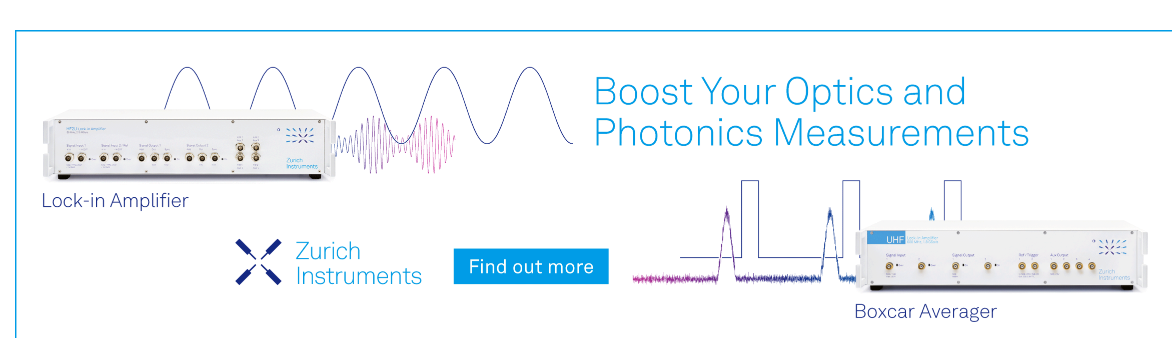

Observation of stacking faults formed during homoepitaxial growth of *p*-type 4*H*-SiC

Ho Keun Song,[1,a)] Jeong Hyun Moon,[2] Hyeong Joon Kim,[2] and Mehran Mehregany[1]
[1]*Department of Electrical Engineering and Computer Science, Case Western Reserve University, Cleveland, Ohio 44106, USA*
[2]*School of Materials Science and Engineering, Seoul National University, Seoul 151-744, Republic of Korea*

(Received 6 October 2008; accepted 6 February 2009; published online 19 March 2009)

Threading dislocations and their transformation into stacking faults (SFs) are observed in *p*-type 4*H*-SiC epitaxial layers by high voltage transmission electron microscope. Homoepitaxial growth and *in situ* aluminum doping of 4*H*-SiC epitaxial layers are carried out using the organosilicon precursor bistrimethylsilylmethane ($C_7H_{20}Si_2$ and the metal-organic precursor trimethylaluminum (C_3H_9Al), and the free hole concentration of the most heavily aluminum-doped epitaxial layers is $>10^{21}$ cm^{-3}. Threading dislocations are formed at the interface between the epitaxial layer and the substrate. However, the density of these threading dislocations decreases toward the epitaxial layer surface with their transformations to SFs. © *2009 American Institute of Physics*.
[DOI: 10.1063/1.3089697]

Silicon carbide (SiC) is a most promising wide band-gap semiconductor for high-power and high-frequency devices because of its excellent electrical and mechanical properties. As a result, SiC has recently been commercialized for high-power devices.[1,2] To date, doping techniques related to *n*-type 4*H*-SiC have been widely researched by a number of groups.[3–8] However, there have been relatively few studies for *p*-type 4*H*-SiC epitaxial growth.[9,10] In the case of the *p*-type 4*H*-SiC epitaxial layers, aluminum (Al) and boron (B) are the most common dopant. Trimethylaluminum (C_3H_9Al, TMA) is usually used as the Al precursor for *in situ* doping. Al atoms are believed to substitute the Si atoms in the SiC lattice.[11,12]

For homoepitaxial growth of *in situ* Al-doped 4*H*-SiC, metal organic chemical vapor deposition with the organosilicon precursor bistrimethylsilylmethane (BTMSM, $C_7H_{20}Si_2$), and metal-organic precursor TMA is used here. BTMSM is nontoxic and nonflammable, thus giving it certain advantages in comparison with using silane (SiH_4). Moreover, because BTMSM has a Si–C bonding structure, low-temperature epitaxial growth is possible.[13–15] TMA is attractive because it is a widely used precursor in the semiconductor industry.

The Al-doped 4*H*-SiC homoepitaxial films were grown on 8° off-axis 4*H*-SiC substrates purchased from Cree, Inc. The deposition temperature and pressure were kept constant at 1370 °C and 180 Torr, respectively. All other growth parameters, except the partial pressure of TMA precursor, were also held constant. The growth rate of the epitaxial layer was about 1 μm/h, and the thickness was about 2 μm. For controlling the Al concentration, the temperature of TMA bath was varied from −15 to 0 °C. High voltage transmission electron microscope (HVTEM, JEOL JEM ARM 1300S) operating at 1.25 MV with point resolution of 1.17 Å was used for observation of crystallographic defects in epitaxial layers. The free hole concentration and mobility were measured by the Hall technique, and the Ohmic contacts at the corners of each sample (6×6 mm^2) were prepared by e-beam evaporation of aluminum with subsequent rapid thermal process annealing.

To examine the effect of Al doping on the crystallinity of the epitaxial layers, the surface morphologies of the Al-doped epitaxial layers were observed by scanning electron microscopy (SEM) and atomic force microscopy (AFM). Figure 1 shows the AFM images (5×5 μm^2) of the surfaces of Al-doped epitaxial layers grown on *p*-type substrates under various TMA partial pressures. The corresponding SEM images are also inserted in each figure. These images illustrate the change in surface morphology with increasing free hole concentration, which changes from 7.5×10^{17} to 2.0×10^{21} cm^{-3}; for TMA partial pressure changes from 3.5×10^{-4} Torr to 1.4×10^{-3} Torr, respectively. In the case of low-doped epitaxial layers grown under a TMA partial pressure of about 10^{-4} Torr [Figs. 1(a) and 1(b)], rms roughness is about few angstrom; SEM images show relatively smooth surfaces. However, the AFM images of the Al-doped epitaxial layers grown under higher TMA partial pressures of about 10^{-3} Torr [Figs. 1(c) and 1(d)] show a step-bunched surface. Macroscopic step bunching prevails throughout the entire area along with the hexagonal arrangement of regular macrosteps [Figs. 1(c) and 1(d)]. These results support the atomic step configuration model proposed by Davis *et al.*[16] The measured step heights were between a few angstrom and 100 Å. The step-bunched surface is thought to be due to Al atoms on the step terraces disturbing the steps flow.

The TMA partial pressure dependence of the 4*H*-SiC (0004) full width half maximum (FWHM) of the rocking curves in the double crystal diffractometry mode was investigated (not shown). In case of *n*-type substrates, the FWHM values were about 20 arc sec before the epitaxial growth. In the undoped epitaxial layer cases, the FWHM values decreased after growth (the FWHM values of the undoped epilayers were about 15 arc sec), but FWHM values of *in situ* Al-doped epitaxial layers increased with increasing TMA partial pressure. In the case of the most heavily doped epilayer, ΔFWHM value was about +10 arc sec (about 30 arc-sec). *In situ* metal doping normally degrades the crystallinity of the epitaxial layers due to the different atomic radii of the

a)Electronic mail: ho-keun.song@case.edu.

18 May 2024 09:54:08

 © 2009 American Institute of Physics

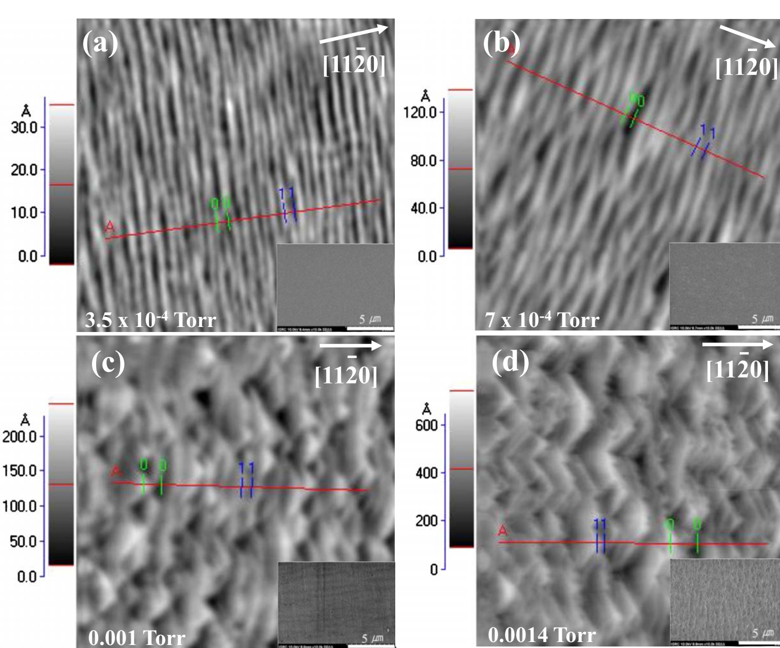

FIG. 1. (Color online) The AFM and SEM images of Al-doped epitaxial layers grown under TMA partial pressures of (a) 3.5×10^{-4}, (b) 7.0×10^{-4}, (c) 0.001, and (d) 0.0014 Torr.

host and the doping atoms (Al in this case) (lattice constant difference=6.3%). So, the stress and strain induced within the SiC lattice result in larger FWHM values. The reciprocal space mapping shows that even the most heavily Al-doped epitaxial layer (TMA partial pressure of 0.002 Torr) has no 3*C*-related peaks (not shown), though it has a somewhat broad ΔQ_y (parallel to $\langle 11\bar{2}0\rangle$ direction of reciprocal space) value due to the mosaicity (lattice tilting) of the epitaxial layer.

To confirm the Al doping effect, cross-sectional HVTEM analysis is carried out. Using the low-magnitude HVTEM images, it is confirmed that the density of stacking faults (SFs) in epitaxial layers increased with increasing TMA partial pressure. Figure 2 shows the low-magnitude bright-field image and high-resolution lattice images of the most heavily Al-doped epitaxial layer (partial pressure of TMA was 0.002 Torr) obtained using HVTEM. The lattice plane shown in Fig. 2 is the $(11\bar{2}0)$ plane. The entire area between interface and surface of the epitaxial layer is observed. Due to its extra-high accelerating voltage (1.25 MeV), HVTEM can penetrate thicker films and give higher resolution than normal TEM. Figure 2(b) shows the bottom part of the epitaxial layer, while Fig. 2(c) shows the upper part of the epitaxial layer [labeled in Fig. 2(a)]. As seen in the low-magnitude bright-field image, there is a high density of threading dislocations at the interface between the substrate and the epitaxial layer. Undoped epitaxial layer do not show these phenomena. The density of threading dislocations decreases toward the surface. These threading dislocations often transform to SFs. The high-resolution lattice image from the bottom part of the epitaxial layer shows that the Al-doped 4*H*-SiC epitaxial layer has a very high density of SFs, which are formed by threading dislocations. However, there are few SFs near the epitaxial layer surface; the high-resolution HVTEM image also shows [Fig. 2(c)] a relatively defect-free 4*H*-SiC lattice. In addition, there is another mechanism that pairs of threading dislocations having Burgers vectors of opposite signs, which are nucleated near the interface, may recombine and disappear because the average distance between dislocation pairs is rather short. Most of the SFs in Fig. 2 are double-Shockley faults, but SFs with irregular stacked number were also observed near the bottom part of the epilayer (including a single-layer Shockley faults).

There are many reports[17–21] on SFs formation in *n*-type 4*H*-SiC, but there appears to be none on SF formation during the growth of *p*-type 4*H*-SiC. In the case of *n*-type 4*H*-SiC, the SFs are formed due to the stress induced by the high nitrogen doping. Therefore, they are observed in highly nitrogen-doped SiC (i.e., where N is over 10^{19} cm^{-3}) after high temperature annealing[20] or oxidation.[21] SFs in SiC are normally formed by the motion of two partial dislocations on the basal plane of the hexagonal SiC. The activation energy for the motion of a partial dislocation is very small, just a

18 May 2024 09:54:08

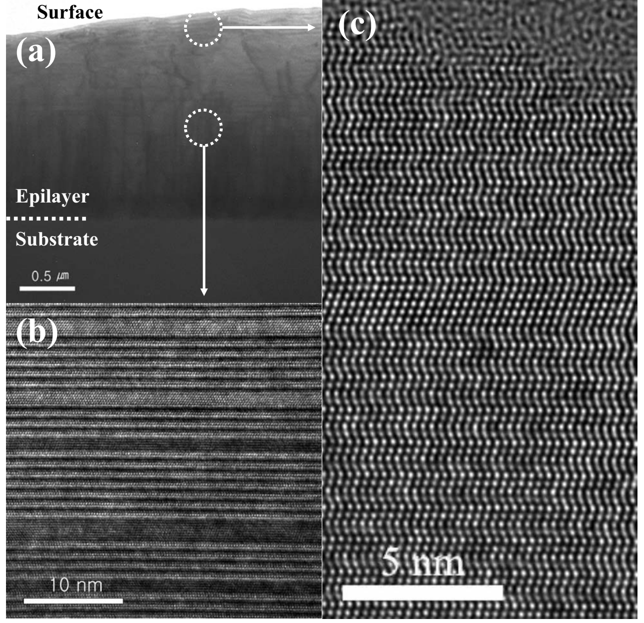

FIG. 2. (a) The low-magnitude bright-field image and [(b) and (c)] high-resolution lattice images of the most heavily Al-doped 4*H*-SiC epitaxial layer using HVTEM (partial pressure of TMA was 0.002 Torr) [(b) shows the bottom part of the epitaxial layer and (c) shows the upper part of the epitaxial layer].

few meV per unit cell. In fact, many researchers have intentionally made SFs by simple heat treatment of highly nitrogen-doped SiC. The formation mechanism of SFs in *p*-type SiC is believed to be the same as that in *n*-type SiC. In addition, because the difference between the atomic radii of the Al and Si is much higher than that between N and C, the stress caused by the doping is much more severe in the case of *p*-type doping. Our samples did not undergo high-temperature heat treatment, which is the driving force of partial dislocations movements. However, the high temperature used during the epitaxial growth itself can cause dislocations movements. From the HVTEM observation, it is clear that the threading dislocations, which are formed at the interface between the epitaxial layer and substrate, can also supply the nucleation site of the partial dislocations for SFs formation in *p*-type SiC. The double-Shockley SFs are formed by the gliding of two partial dislocations in adjacent basal planes of 4*H*-SiC and, due to the component parallel to the basal plane of hexagonal SiC in Burgers vector of threading dislocations, basal plane dislocations (partial dislocations with a Burgers vector $a/3\langle 10\bar{1}0\rangle$) glide down over the (0001) plane. The motion of these basal plane dislocations results in SFs. On the contrary, the threading dislocations continuously lose their energy and finally disappear as shown in Fig. 2(a). From these results, it is clear that the stress in the lattice of 4*H*-SiC, which is generated due to the heavy Al doping, can be released by the formation of threading dislocations on the interface and their transform into SFs during the crystal growth.

The free hole concentration and mobility in the Al-doped *p*-type epitaxial layers are measured by the Hall measurement system (not shown). The free hole concentration increases with increasing TMA partial pressure. By contrast, the mobility of the free holes decreases with increasing free hole concentration. The high quality of the epitaxial layers is documented by the high values of hole mobility, which range from 0.13 to 78 $cm^2/V\ s$ at room temperature for free hole concentration from 2.0×10^{21} to $7.5\times10^{17}\ cm^{-3}$, respectively.

In conclusion, the HVTEM results show that many threading dislocations were formed at the interface between the substrate and the epitaxial layer during the epitaxial growth. These threading dislocations were transformed into SFs during crystal growth. In addition, the density of the threading dislocations decreased toward the epitaxial layer surface. It is assumed that the transformation from threading dislocations to SFs is a stress release mechanism in the heavily aluminum-doped *p*-type SiC.

This work was supported by the Korea Research Foundation Grant funded by the Korean Government (MOEHRD) (Grant No. KRF-2007-357-D00117).

[1]See http://www.cree.com for more information about the commercial SiC power devices.
[2]See http://www.infineon.com for more information about the commercial SiC power devices.
[3]J. Pernot, S. Contreras, J. Camassel, J. L. Robert, W. Zawadzki, E. Neyret, and L. Di Cioccio, Appl. Phys. Lett. **77**, 4359 (2000).
[4]H. Iwata and K. M. Itoh, J. Appl. Phys. **89**, 6228 (2001).
[5]J. Pernot, W. Zawadzki, S. Contreras, J. L. Robert, E. Neyret, and L. Di Cioccio, J. Appl. Phys. **90**, 1869 (2001).
[6]R. Wang, I. B. Bhat, and T. P. Chow, J. Appl. Phys. **92**, 7587 (2002).
[7]T. Kimoto, T. Yamamoto, Z. Y. Chen, H. Yano, and H. Matsunami, J. Appl. Phys. **89**, 6105 (2001).
[8]J. Jeong, H. Song, M. Um, H. Na, I. Song, and H. Kim, J. Electrochem. Soc. **151**, G252 (2004).
[9]A. Kakanakova-Georgieva, R. Yakimova, M. K. Linnarsson, and E. Janzén, J. Appl. Phys. **91**, 3471 (2002).
[10]B. E. Landini and G. R. Brandes, Appl. Phys. Lett. **74**, 2632 (1999).
[11]T. Kimoto, S. Nakazawa, K. Fujihira, T. Hirao, S. Nakamura, Y. Chen, K. Hashimoto, and H. Matsunami, Mater. Sci. Forum **389**, 165 (2002).
[12]G. Wagner, W. Leitenberger, K. Irmscher, F. Schmid, M. Laube, and G. Pensl, Mater. Sci. Forum **389**, 207 (2002).
[13]W. Bahng and H. Kim, Appl. Phys. Lett. **69**, 4053 (1996).
[14]H. Song, S. Kwon, H. Seo, J. Moon, J. Yim, J. Lee, H. Kim, and J. Jeong, Appl. Phys. Lett. **89**, 152112 (2006).
[15]H. Song, H. Seo, S. Kwon, J. Moon, J. Yim, J. Lee, and H. Kim, J. Cryst. Growth **305**, 83 (2007).
[16]R. F. Davis, S. Tanaka, R. S. Kern, J. Xu, and J. F. Wendelken, Inst. Phys. Conf. Ser. **142**, 133 (1996).
[17]R. S. Okojie, M. Zhang, and P. Pirouz, Mater. Sci. Forum **457**, 529 (2004).
[18]M. S. Miao, S. Limpijumnong, and W. L. Lambrecht, Appl. Phys. Lett. **79**, 4360 (2001).
[19]A. Galeckas, J. Linnros, and P. Pirouz, Phys. Rev. Lett. **96**, 025502 (2006).
[20]T. A. Kuhr, J. Liu, H. Chung, M. Skowronski, and F. Szmulowicz, J. Appl. Phys. **92**, 5863 (2002).
[21]R. S. Okojie, M. Xhang, P. Pirouz, S. Tumakha, G. Jessen, and L. J. Brillson, Appl. Phys. Lett. **79**, 3056 (2001).

18 May 2024 09:54:08